SCF$^{\beta TrCP}$ mediates stress-activated MAPK-induced Cdc25B degradation

JCS083931 Supplementary Material

Files in this Data Supplement:

- **Supplemental Figure S1 - Fig. S1. SCFβTrCP ubiquitylates Cdc25B.** (A) 35S-methione-labelled Cdc25BDAA of human B1, human B3, and mouse B1 was incubated with the SCFβTrCP complex in the presence or absence of JNK1, and the ubiquitylation was determined as described in the *Materials and Methods*. The ubiquitylation of 35S-methione-labelled Cdc25B1DAA with additional mutations of D94A or S101/103A was also determined. (B) The following FLAG-Cdc25BDAA-based mutants were cotransfected with Myc-βTrCP1 in the presence or absence of JNK1: WT without other mutation; S101A; S103A; S101/103A; or D94A. Then, 24 h later, Cdc25B-bound βTrCP1 was detected by the immunoprecipitation of Cdc25B, followed by immunoblotting (Cdc25B-IP panel). The expression of the indicated proteins is also shown (WCE panel).
- **Supplemental Figure S2 - Fig. S2. The depletion of βTrCP1/2 with siRNA stabilises Cdc25B.** (A) HeLa cells constitutively expressing FLAG-Cdc25B (HeLa-W40 cells) were transfected with control siRNA (against luciferase (Luci)) or siRNA that targets both βTrCP1 and βTrCP2 (βTrCP). After 24 h, the expression of FLAG-Cdc25B, endogenous Cdc25A, βTrCP1, and β-actin was determined by immunoblotting. (B) HeLa cells were transfected with siRNA against luciferase (Luci) or βTrCP (pan-βTrCP or βTrCP1 + 2). After 24 h, these cells were further transfected with FLAG-Cdc25BDAA with or without JNK1 and MKK7. After 24 h, the expression of Cdc25BDAA and the indicated proteins was determined by immunoblotting. (C) HeLa-DAA34 cells expressing FLAG-Cdc25BDAA were transfected with siRNA against either Luci or pan-βTrCP and challenged with 50 ng/mL anisomycin. The expression of the indicated proteins was determined by immunoblotting at the indicated time points. Quantitative results for the expression of

Cdc25BDAA are shown. The results shown are the average of three independent experiments with the SD.

- **Supplemental Figure S3 - Fig. S3. Cdc25B S101 and S103 are phosphorylated by JNK or by UV irradiation.** (A) The specificity of phospho-specific antibodies was evaluated using *in vitro* phosphorylated Cdc25B. The GST-fused Cdc25B N-terminal fragment (1−175) purified from *E. coli* was phosphorylated by JNK1 and probed with the indicated antibodies. (B) HeLa-W40 cells were irradiated with UV at 20 J/m2, and cell extracts were prepared at the indicated times. After the immunoprecipitation of Cdc25B with anti-FLAG beads, the phosphorylation status of the indicated amino acids was determined by immunoblotting with each phospho-specific antibody. The expression of the indicated proteins is also shown.
- **Supplemental Figure S4 - Fig. S4. p38 and JNK are involved in phosphorylation at S101 and S103.** HeLa-W40 cells were treated with the p38 inhibitor SB202190 (A), p38 inhibitor PD169316 (B), or JNK inhibitor SP600125 (C) at the indicated concentration 1 h before the challenge with 50 ng/mL anisomycin. FLAG-Cdc25B was recovered with anti-FLAG agarose beads, and then the expression and phosphorylation of S101 or S103 was determined by immunoblotting with specific antibodies. The expression of other proteins was also determined. (D) HeLa cells were transfected with the wild-type or kinase-dead form of JNK1 with MKK7. After 24 h, the expression of endogenous Cdc25B was determined by immunoprecipitation followed by immunoblotting. The expression of the indicated proteins is also shown. The transfection efficiency of JNK1 was about 75% (range 70−80%).
- **Supplemental Figure S5 - Fig. S5. Cdc25B DAG mutations stabilise Cdc25B.** (A) FLAG-Cdc25B of the wild type or D94A, G96A, or S101/103A mutants was cotransfected with or without JNK1. The expression of the indicated proteins was determined 24 h after transfection by immunoblotting. (B) Cdc25B of the wild type, D94A, or S101/103A was cotransfected with or without JNK1. After 24 h, cell extracts were prepared, and Cdc25B was immunoprecipitated with

anti-FLAG beads, followed by the determination of Cdc25B S101/103 phosphorylation by immunoblotting.

- **Supplemental Figure S6 - Fig. S6. The Cdc25B PEST-like sequence plays an important role in JNK-induced degradation**. (A) FLAG-Cdc25B of the wild-type or PEST-like sequence mutant (all eight serine residues in the PEST-like sequence were mutated to alanine, 8SA -PEST), S101/103A, or D94A mutants were transfected into HeLa cells in the presence or absence of JNK1. The expression of the indicated proteins was determined 24 h after transfection. (B) FLAG-Cdc25B of the wild-type or PEST-like sequence mutants in which different numbers of serine residues were mutated to alanine were transfected to HeLa cells with or without JNK1. The expression of the indicated proteins was determined 24 h after transfection. (C) FLAG-Cdc25B mutants with mutations in two serine residues in each ESS unit or in LSS in the PEST-like sequence were transfected with or without JNK1. The expression of the indicated proteins was determined 24 h after transfection. (D) FLAG-Cdc25B of wild type or the E88A, E91A, or D94A mutant was transfected with or without JNK1. The expression of the indicated proteins was determined 24 h after transfection. (E) Cdc25B of the wild type, 8SA (-PEST), S101/103A, or D94A was cotransfected with or without JNK1. After 24 h, cell extracts were prepared, and Cdc25B was immunoprecipitated with anti-FLAG beads, followed by the determination of Cdc25B S101/103 phosphorylation by immunoblotting.

Supplemental Figure S7 - Fig. S7. DAG is a JNK-dependent βTrCP1 site in Cdc25B and DDG is a JNK-independent site. FLAG-Cdc25B of the wild type or D94A, DAA, or D94A/DAA mutants was transfected with or without JNK1. After 24 h, the FLAG-Cdc25B proteins were recovered by immunoprecipitation and the βTrCP1 bound to FLAG-Cdc25B or recovered FLAG-Cdc25B was determined by immunoblotting (Cdc25B-IP). The expression of the indicated proteins 24 h after transfection is also shown (WCE).

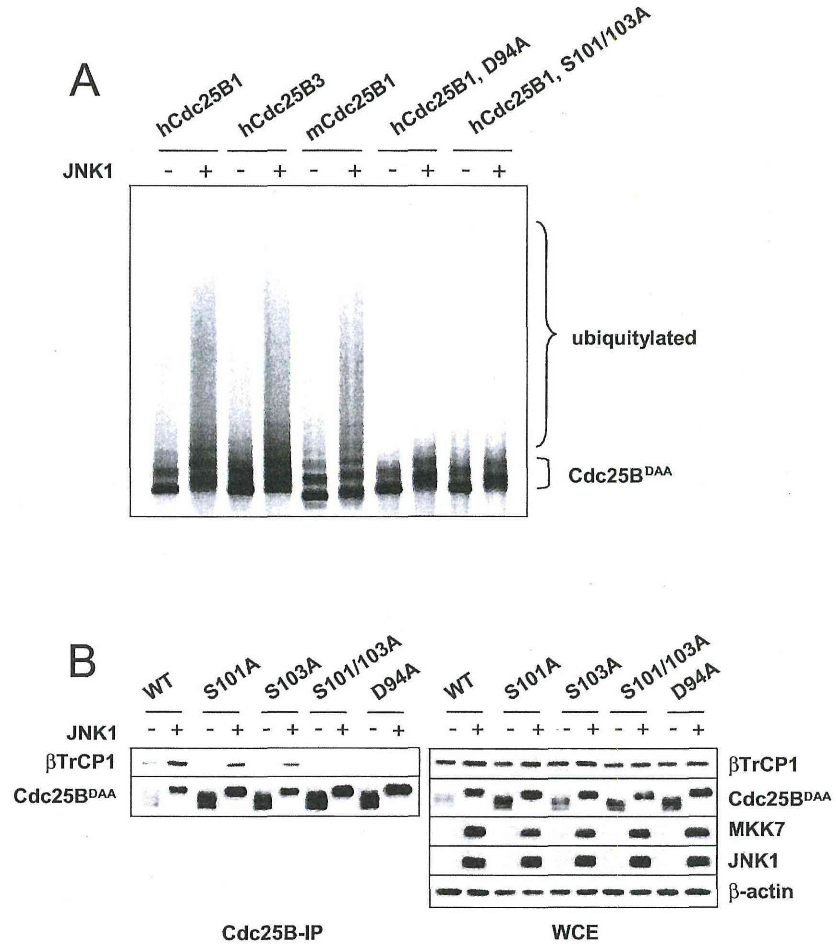
A
hCdc25B1
hCdc25B3
mCdc25B1
hCdc25B1, D94A
hCdc25B1, S101/103A
JNK1
ubiquitylated
Cdc25B^DAA
B
WT
S101A
S103A
S101/103A
D94A
JNK1
βTrCP1
Cdc25B^DAA
MKK7
β-actin
Cdc25B-IP
WCE

Fig. S1

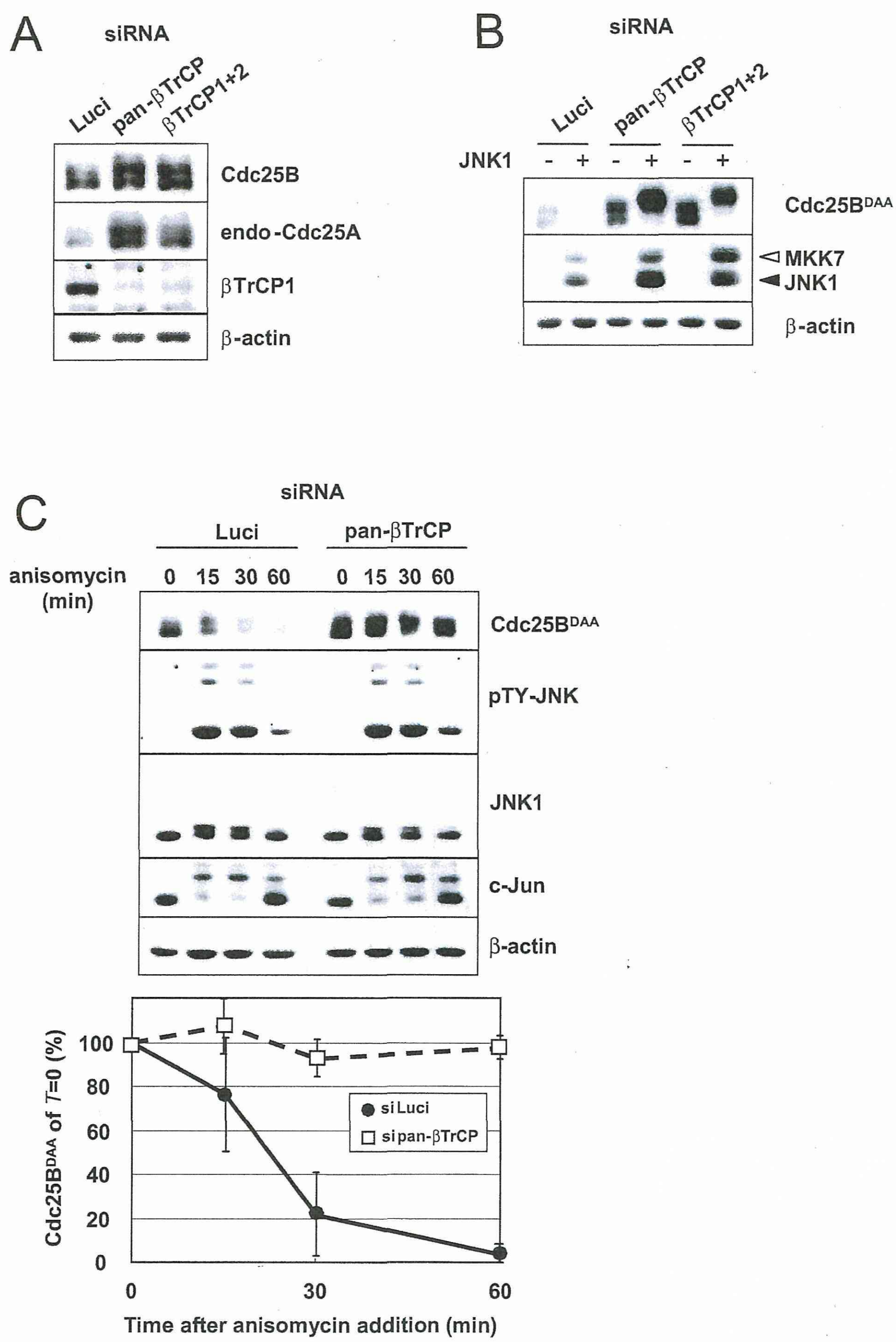
A
siRNA
Luci
pan-βTrCP
βTrCP1+2
Cdc25B
endo-Cdc25A
βTrCP1
β-actin
B
siRNA
Luci
pan-βTrCP
βTrCP1+2
JNK1
- + - + - +
Cdc25BDAA
MKK7
JNK1
β-actin
C
siRNA
Luci
pan-βTrCP
anisomycin (min)
0 15 30 60 0 15 30 60
Cdc25BDAA
pTY-JNK
JNK1
c-Jun
β-actin
Cdc25BDAA of T=0 (%)
100
80
60
40
20
0
0
30
60
Time after anisomycin addition (min)
siLuci
sipan-βTrCP

Fig. S2

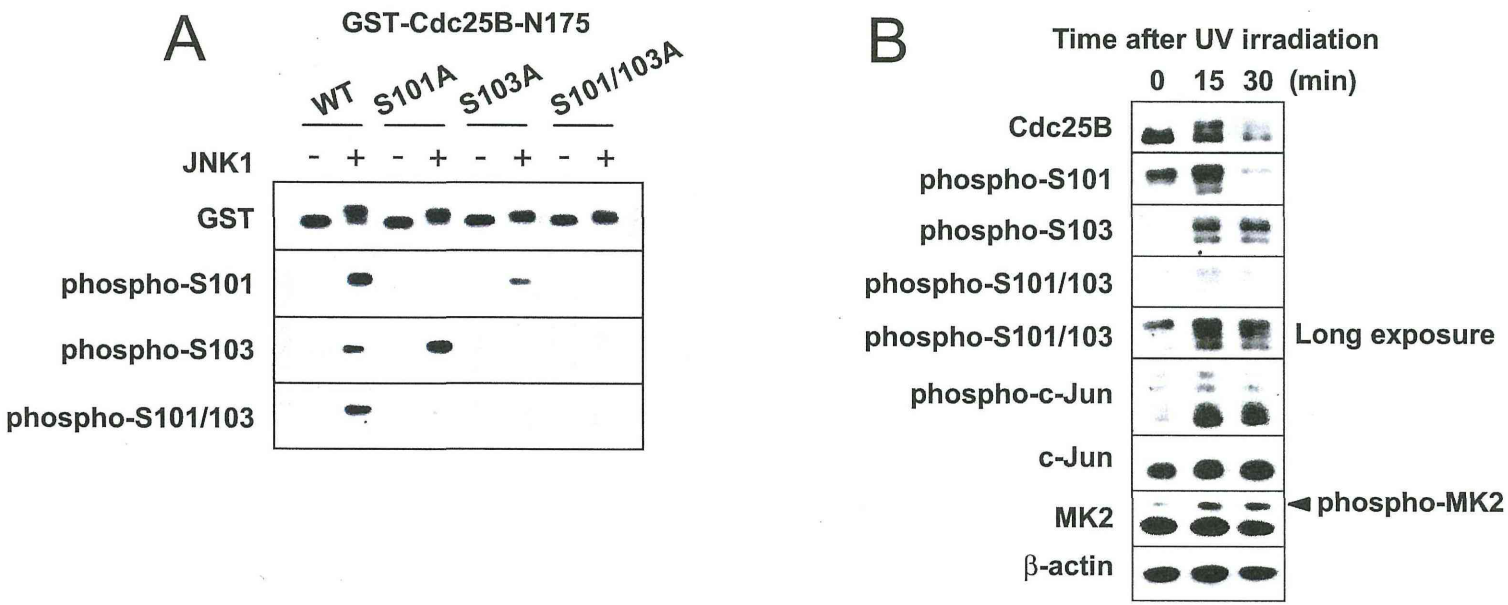
A
GST-Cdc25B-N175
WT
S101A
S103A
S101/103A
JNK1
- + - + - + - +
GST
phospho-S101
phospho-S103
phospho-S101/103
B
Time after UV irradiation
0 15 30 (min)
Cdc25B
phospho-S101
phospho-S103
phospho-S101/103
phospho-S101/103
Long exposure
phospho-c-Jun
c-Jun
MK2
phospho-MK2
β-actin

Fig. S3

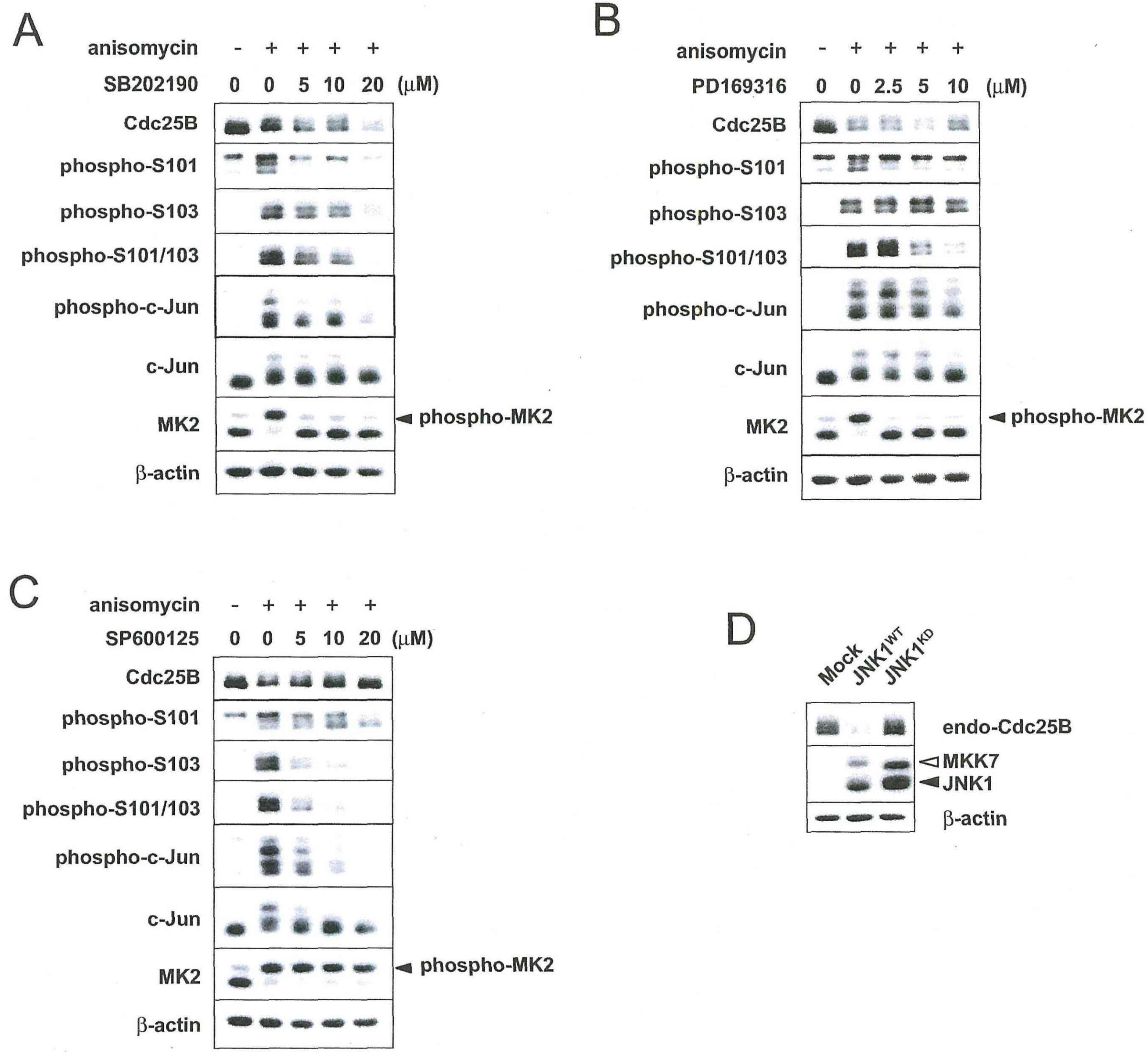
A
anisomycin - + + + +
SB202190 0 0 5 10 20 (μM)
Cdc25B
phospho-S101
phospho-S103
phospho-S101/103
phospho-c-Jun
c-Jun
MK2
phospho-MK2
β-actin
B
anisomycin - + + + +
PD169316 0 0 2.5 5 10 (μM)
Cdc25B
phospho-S101
phospho-S103
phospho-S101/103
phospho-c-Jun
c-Jun
MK2
phospho-MK2
β-actin
C
anisomycin - + + + +
SP600125 0 0 5 10 20 (μM)
Cdc25B
phospho-S101
phospho-S103
phospho-S101/103
phospho-c-Jun
c-Jun
MK2
phospho-MK2
β-actin
D
Mock
JNK1WT
JNK1KD
endo-Cdc25B
MKK7
JNK1
β-actin

Fig. S4

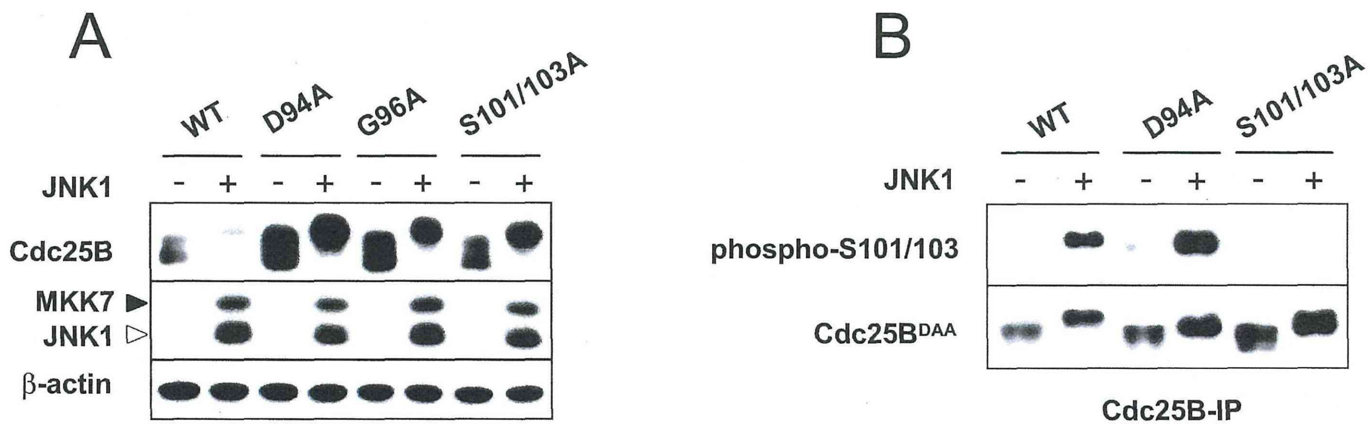
A
WT
D94A
G96A
S101/103A
JNK1
- + - + - + - +
Cdc25B
MKK7
JNK1
β-actin
B
WT
D94A
S101/103A
JNK1
- + - + - +
phospho-S101/103
Cdc25BDAA
Cdc25B-IP

Fig. S5

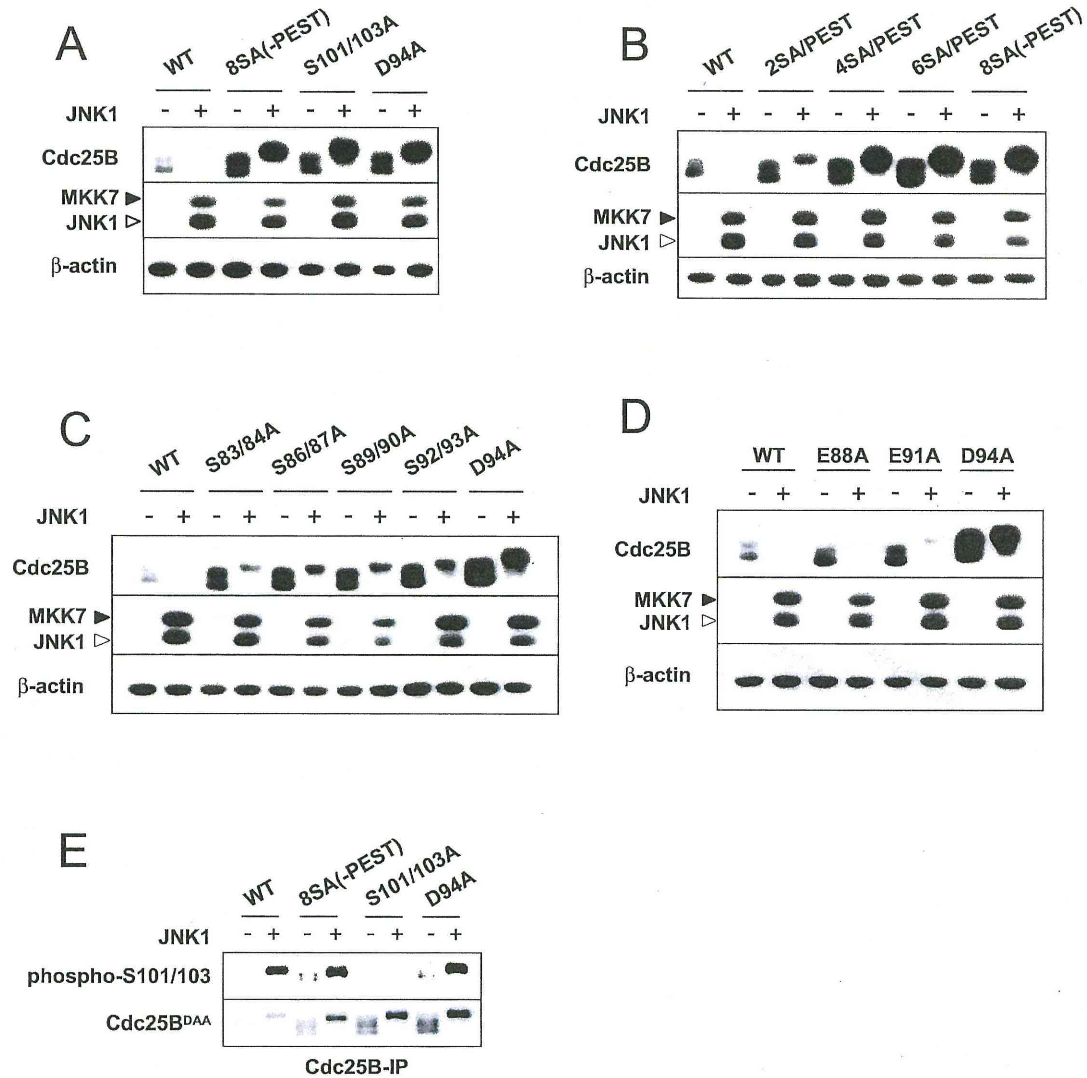
A
WT
8SA(-PEST)
S101/103A
D94A
JNK1
Cdc25B
MKK7
JNK1
β-actin
B
WT
2SA/PEST
4SA/PEST
6SA/PEST
8SA(-PEST)
JNK1
Cdc25B
MKK7
JNK1
β-actin
C
WT
S83/84A
S86/87A
S89/90A
S92/93A
D94A
JNK1
Cdc25B
MKK7
JNK1
β-actin
D
WT
E88A
E91A
D94A
JNK1
Cdc25B
MKK7
JNK1
β-actin
E
WT
8SA(-PEST)
S101/103A
D94A
JNK1
phospho-S101/103
Cdc25BDAA
Cdc25B-IP

Fig. S6

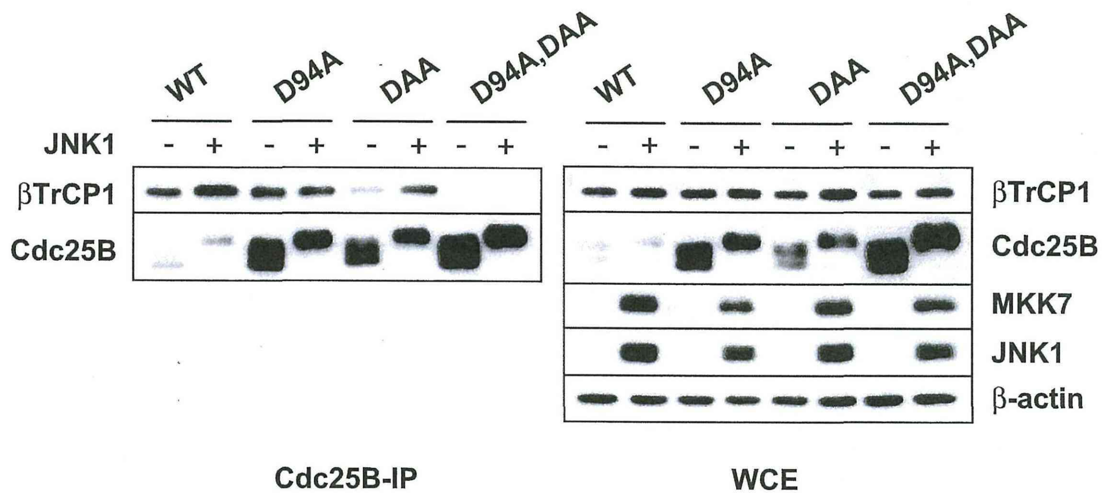
WT
D94A
DAA
D94A,DAA
WT
D94A
DAA
D94A,DAA
JNK1
- + - + - + - +
- + - + - + - +
βTrCP1
Cdc25B
βTrCP1
Cdc25B
MKK7
JNK1
β-actin
Cdc25B-IP
WCE

Fig. S7

Oncogene (2011) 1–12

www.nature.com/onc

ORIGINAL ARTICLE

Inflammation-induced repression of tumor suppressor miR-7 in gastric tumor cells

D Kong[1,7], Y-S Piao[1,7,8], S Yamashita[2], H Oshima[1], K Oguma[1], S Fushida[3], T Fujimura[3], T Minamoto[4], H Seno[5], Y Yamada[6], K Satou[6], T Ushijima[2], T-O Ishikawa[1] and M Oshima[1]

[1]*Division of Genetics, Cancer Research Institute, Kanazawa University, Kanazawa, Japan;* [2]*Division of Epigenomics, National Cancer Center Research Institute, Tokyo, Japan;* [3]*Department of Gastroenterologic Surgery, Kanazawa University Hospital, Kanazawa, Japan;* [4]*Division of Translational and Clinical Oncology, Cancer Research Institute, Kanazawa University, Kanazawa, Japan;* [5]*Department of Gastroenterology and Hepatology, Kyoto University Graduate School of Medicine, Kyoto, Japan and* [6]*Faculty of Electrical and Computer Engineering, Institute of Science and Engineering, Kanazawa University, Kanazawa, Japan*

Inflammation has an important role in cancer development through various mechanisms. It has been shown that dysregulation of microRNAs (miRNAs) that function as oncogenes or tumor suppressors contributes to tumorigenesis. However, the relationship between inflammation and cancer-related miRNA expression in tumorigenesis has not yet been fully understood. Using *K19-C2mE* and *Gan* mouse models that develop gastritis and gastritis-associated tumors, respectively, we found that 21 miRNAs were upregulated, and that 29 miRNAs were downregulated in gastric tumors in an inflammation-dependent manner. Among these miRNAs, the expression of miR-7, a possible tumor suppressor, significantly decreased in both gastritis and gastric tumors. Moreover, the expression of miR-7 in human gastric cancer was inversely correlated with the levels of interleukin-1β and tumor necrosis factor-α, suggesting that miR-7 downregulation is related to the severity of inflammatory responses. In the normal mouse stomach, miR-7 expression was at a basal level in undifferentiated gastric epithelial cells, and was induced during differentiation. Moreover, transfection of a miR-7 precursor into gastric cancer cells suppressed cell proliferation and soft agar colony formation. These results suggest that suppression of miR-7 expression is important for maintaining the undifferentiated status of gastric epithelial cells, and thus contributes to gastric tumorigenesis. Although epigenetic changes were not found in the CpG islands around miR-7-1 of gastritis and gastric tumor cells, we found that activated macrophage-derived small molecule(s) (<3 kDa) are responsible for miR-7 repression in gastric cancer cells. Furthermore, the miR-7 expression level significantly decreased in the inflamed gastric mucosa of *Helicobacter*-infected mice, whereas it increased in the stomach of germfree *K19-C2mE* and *Gan* mice wherein inflammatory responses were suppressed. Taken together, these results indicate that downregulation of tumor suppressor miR-7 is a novel mechanism by which the inflammatory response promotes gastric tumorigenesis.
Oncogene advance online publication, 5 December 2011; doi:10.1038/onc.2011.558

Keywords: miR-7; gastric cancer; inflammation; macrophages

Correspondence: Professor M Oshima, Division of Genetics, Cancer Research Institute, Kanazawa University, Kakuma-machi, Kanazawa, 920-1192, Japan.
E-mail: oshimam@kenroku.kanazawa-u.ac.jp
[7]These authors contributed equally to this work.
[8]Current address: Department of Pathophysiology, Medical College, Yanbian University, Yanji City 133002, China.
Received 18 July 2011; revised 22 October 2011; accepted 2 November 2011

Introduction

It has been established that inflammatory responses contribute to cancer development through various mechanisms (Coussens and Werb, 2002). The expression of cyclooxygenase-2 (COX-2), a rate-limiting enzyme for prostaglandin biosynthesis, has an important role in both inflammation and cancer (Wang and DuBois, 2010). Using genetic mouse models, we previously demonstrated that induction of COX-2 and its downstream product, prostaglandin E_2 (PGE_2), is required for gastrointestinal tumorigenesis (Sonoshita *et al.*, 2001; Oshima *et al.*, 2006). The COX-2/PGE_2 pathway, together with a bacterial infection, induces inflammatory responses in the stomach through the recruitment of macrophages, which promotes gastric tumorigenesis (Oshima *et al.*, 2011). However, it remains to be fully elucidated precisely how such inflammatory responses contribute to the promotion of gastric tumors.

MicroRNAs (miRNAs) are a class of single-stranded small noncoding RNAs that regulate gene expression by post-transcriptional interference of specific mRNAs (Ambros, 2004; Bartel, 2004). Through their regulation of cancer-related gene expression, miRNAs can function as either oncogenes or tumor suppressors (Esquela-Kerscher and Slack, 2006; Ventura and Jacks, 2009). Dysregulation of miRNAs in cancer has been shown to be associated with genomic/epigenetic alterations or transcriptional/post-transcriptional mechanisms (Di Leva and Croce, 2010). Moreover, expression of several miRNAs, including oncogenic miRNAs, has been shown to be induced by inflammatory responses (Sonkoly and Pivarcsi, 2011). For example, miR-155 is induced in macrophages by nuclear factor-κB, interferon-β or Toll-like receptor signaling (O'Connell *et al.*, 2007; Tili *et al.*, 2007), whereas miR-21 is induced by Stat3, a transcription factor activated by interleukin-6 (IL-6) (Iliopoulos *et al.*, 2010). On the other hand, the mechanism responsible for the downregulation of tumor-suppressor miRNA expression in the inflammatory microenvironment has not been fully understood.

Herein, we examined the expression of miRNAs in mouse models of gastritis and gastric tumors, which were developed in *K19-C2mE* and *Gan* mice, respectively (Oshima *et al.*, 2004, 2006). We found the expression level of miR-7 to significantly decrease in gastric tumors in an inflammation-dependent manner. It has been shown that miR-7 has a tumor-suppressor role in several cancers, including glioblastoma, breast cancer and lung cancer (Kefas *et al.*, 2008; Reddy *et al.*, 2008; Webster *et al.*, 2009; Jiang *et al.*, 2010; Saydam *et al.*, 2011). In this manuscript, we demonstrate that miR-7 is induced during the differentiation of normal gastric epithelial cells, and it also has a tumor-suppressor role in the stomach. These results suggest that downregulation of tumor suppressor miR-7 is one of the tumor-promoting mechanisms underlying the role of inflammation in gastric tumorigenesis.

Results

Inflammation-dependent dysregulation of miRNAs in gastric tumors

To examine whether miRNA expression is dysregulated in gastric tumors by inflammatory responses, we examined the miRNA expression profiles in wild-type mouse stomachs, *K19-C2mE* mouse gastritis and *Gan* mouse gastric tumors by a microarray analysis. In *Gan* mouse gastric tumors, 50 miRNAs were upregulated (>2.0-fold), whereas 42 miRNAs were downregulated (<0.5-fold) compared with the wild-type mouse stomach level (Figure 1a and Supplementary Table 1). Notably, 21 and 29 miRNAs showed upregulation or downregulation, respectively, in both gastritis and gastric tumors. Therefore, it is possible that dysregulation of these miRNAs is caused by inflammatory responses.

We confirmed the results of the microarray analysis by real-time reverse transcriptase–polymerase chain reaction (RT–PCR). In all, 10 miRNAs randomly selected from the upregulated and downregulated miRNAs (Figure 1a, boxed) showed the same dysregulation pattern in both gastritis and gastric tumors (Figure 1b). Importantly, miR-155 and miR-21, which function as oncogenes (Volinia *et al.*, 2006) were upregulated, whereas miR-145 and miR-7, which function as tumor suppressors (Kefas *et al.*, 2008; Sachdeva *et al.*, 2009), were downregulated in both gastritis and gastric tumors (Figures 1a and b). This suggests that inflammation can induce not only upregulation of oncogenic miRNAs but also downregulation of tumor-suppressor miRNAs.

We next picked up 74 miRNAs that were not dysregulated in *K19-C2mE* gastritis compared with the wild-type normal stomach (Supplementary Table 2). Among them, three miRNAs were upregulated in *Gan* mouse tumors compared with *K19-C2mE* gastritis tissue samples (>2.0-fold), whereas three miRNA were downregulated (<0.5-fold) (Figure 1c). It is possible that expression of these miRNAs is dysregulated by carcinogenesis-specific mechanisms.

Induction of miR-7 during differentiation of gastric epithelial cells

We further examined the expression of miR-7, because its role(s) in the normal stomach and gastric cancer have never been examined. Gastric glands were isolated from the stomachs of the respective mouse models, and the miR-7 expression was examined by real-time RT–PCR. Notably, miR-7 levels were significantly lower in epithelial cells of *K19-C2mE* gastritis tissues and *Gan* mouse tumors compared with the wild-type mouse stomach (Figure 2a), indicating that miR-7 is predominantly expressed in epithelial cells in an inflammation-dependent manner.

When primary cultured gastric epithelial cells were passaged and maintained for 6 days, the cell morphology appeared to be differentiated, with enlarged and mucin-containing cytoplasm (Figure 2b). Consistently, the expression of differentiation markers, *Muc6* and *Muc5AC*, was elevated on day 6, whereas the expression of the Wnt target gene, *Sox9*, decreased (Figure 2c). These results indicate that cultured gastric epithelial cells underwent differentiation through passage and 6-day culture. Importantly, the miR-7 expression level increased significantly on day 6 to 6.5-fold, compared with the level observed on day 2.

We next examined the miR-7 level in the stomach during development. The expression level of miR-7 in the stomach increased significantly in 14-day-old and adult mice, to >6-fold of that in E15 embryos (Figure 2d). Conversely, expression of *CD44*, one of the Wnt target genes, decreased significantly during development. We confirmed by an immunohistochemistry that most epithelial cells in the gastric mucosa were Ki-67 positive on days 0 and 7, whereas proliferating cells were limited to the gland neck on day 14 and in adult mice (Figure 2e). Accordingly, the ratio of undifferentiated epithelial cells decreased during development. Taken together, these results indicate that miR-7 expression is induced in gastric epithelial cells during differentiation.

Tumor-suppressor role of miR-7 in gastric cancer development

We next examined miR-7 levels in human gastric cancers by real-time RT–PCR. The expression of miR-7 was downregulated in 18 out of 28 human gastric cancer tissue samples (64%) compared with paired non-tumor stomach tissue samples (Figure 3a), suggesting that miR-7 has a tumor-suppressor role in a subpopulation of gastric cancers. We next examined the expression

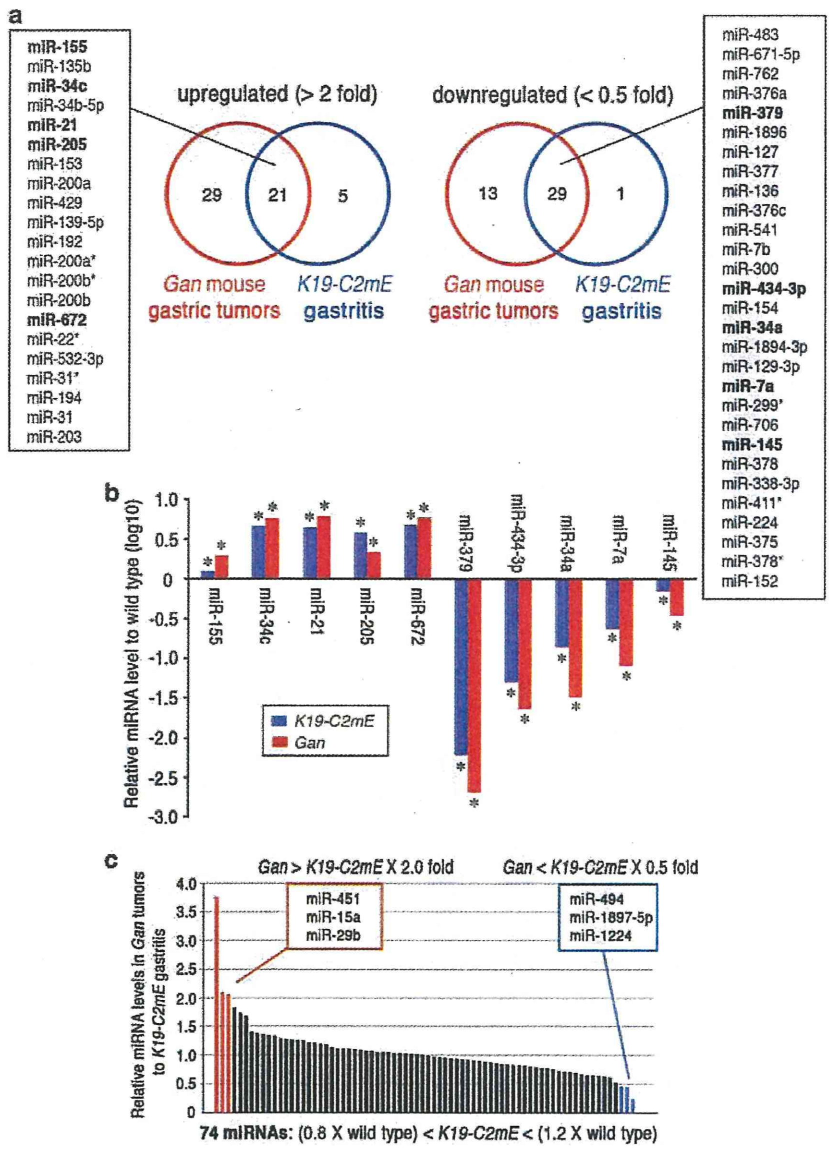

Figure 1 Inflammation-dependent dysregulation of miRNA expression in mouse gastric tumors. (**a**) Venn diagrams of the miRNAs that were upregulated (>2.0) and downregulated (<0.5) in *Gan* mouse gastric tumors and/or *K19-C2mE* mouse gastritis samples as determined by the microarray analysis are shown. The miRNAs listed in boxes were upregulated (left) or downregulated (right) in both gastric tumor and gastritis tissue samples. (**b**) The relative expression levels of selected miRNAs (indicated in bold in the list) for *K19-C2mE* mouse gastritis (blue bars) and *Gan* mouse gastric tumors (red bars) compared with the wild-type levels examined by real-time RT–PCR are shown as the log10 ratios. **P*<0.05 versus the wild-type level. The expression levels of miRNAs were normalized to the Sno202 level. (**c**) The miRNA levels in *Gan* mouse tumors relative to those in *K19-C2mE* gastritis tissues examined by the microarray analysis are shown. Red and blue bars indicate upregulated (>2.0) and downregulated (<0.5) miRNAs, respectively, in *Gan* mouse tumors.

level of IL-1β and tumor necrosis factor (TNF)-α, major proinflammatory cytokines, and compared them with the miR-7 level. Importantly, expression levels of miR-7 were inversely correlated with those of IL-1β or TNF-α, suggesting that the downregulation of miR-7 is related to the severity of inflammatory responses (Figure 3b). We also found that miR-7 was markedly downregulated in four out of nine gastric cancer cells lines (Figure 3c).

To examine the tumor-suppressor role of miR-7 in gastric tumorigenesis, we transfected the precursor of miR-7, pre-miR-7, into AZ-521 and Kato-III gastric cancer cells and examined their proliferation and soft agar colony formation. We confirmed that pre-miR-7 transfection into reporter vector-transfected cells resulted in a significant decrease in luciferase activity, indicating an increase of mature miR-7 level (Supplementary Figure 1). Transfection of pre-miR-7

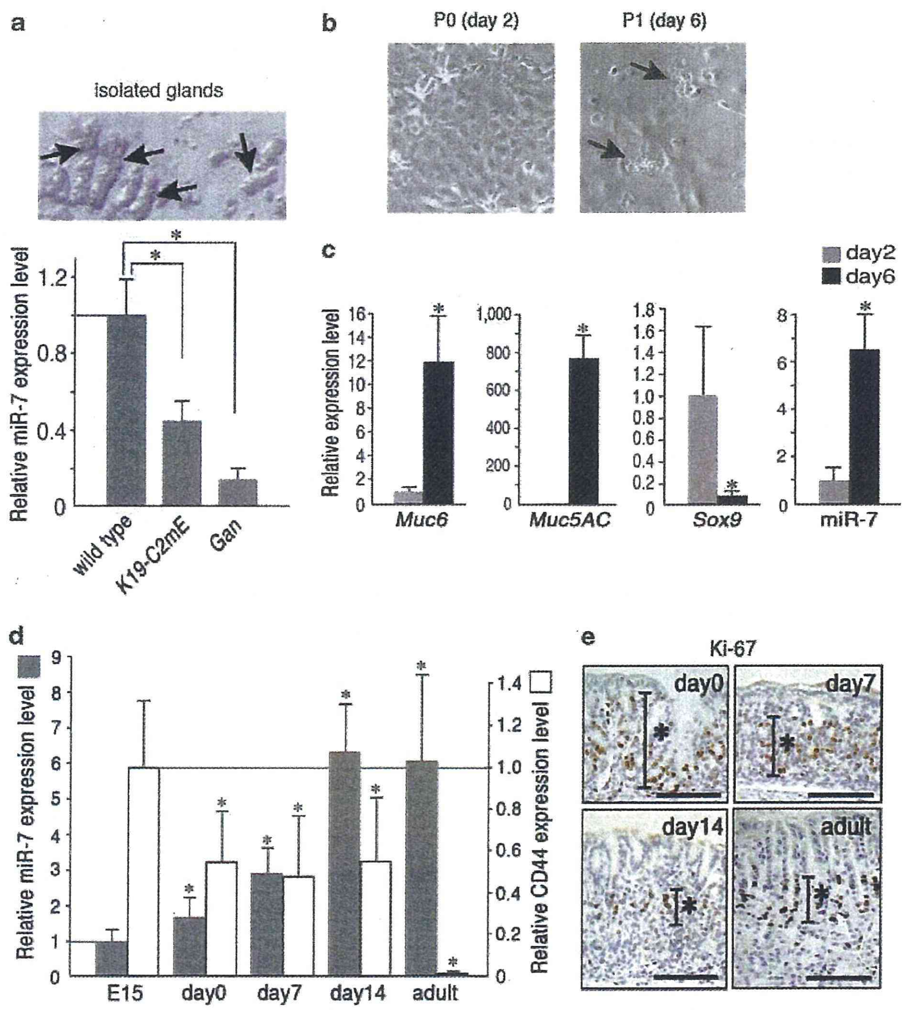

Figure 2 The induction of miR-7 expression in differentiated gastric epithelial cells. (**a**) A representative photograph of isolated gastric glands from wild-type mice (top, arrows). The expression levels of miR-7 in the isolated gastric glands of *K19-C2mE* and *Gan* mice relative to the wild-type level are shown (mean ± s.d.) (bottom). $*P<0.05$. (**b**) Representative photographs of primary cultured gastric epithelial cells on day 2 (passage 0: P0) and on day 6 (passage 1: P1) (original magnification, × 100). Arrows in P1 indicate mucin-containing enlarged cells on day 6. (**c**) The levels of *Muc6*, *Muc5AC* and *Sox9* mRNA and miR-7 in the primary cultured gastric epithelial cells on day 6 (closed bars) relative to the levels on day 2 (gray bars) are shown (mean ± s.d.). $*P<0.05$ versus the day 2 level. (**d**) The expression levels of miR-7 (gray bars) and *CD44* (open bars) in the stomach at the indicated ages relative to the levels in E15 embryos are shown (mean ± s.d.). $*P<0.05$ versus the E15 level. The expression levels of miR-7 were normalized to the Sno202 level. (**e**) Representative photographs of Ki-67 immunostaining in the glandular stomach of mice at the indicated ages. Asterisks indicate proliferative zones. Scale bars indicate 50 μm.

significantly decreased cell proliferation in both cell lines compared with control vector-transfected cells (Figure 3d). Moreover, pre-miR-7 transfection significantly suppressed soft agar colony formation in both cell lines (Figures 3e and f). These results strongly suggest that miR-7 has a tumor-suppressor role in gastric cancer development.

Repression of miR-7 in gastric cancer cells by macrophage-derived factor(s)

We detected primary (pri)-miR-7-1, pri-miR-7-2 and pri-miR-7b in the mouse normal stomach by real-time RT–PCR (Supplementary Figure 2), suggesting that mature miR-7 is processed from all these primary miR-7 in the normal gastric mucosa. MiR-7-1 is located in the intron of the *Hnrnpk* gene, and a CpG island is found in the promoter region of *Hnrnpk* (Supplementary Figure 3a). On the other hand, we could not determine CpG islands that regulate the transcription of miR-7-2 and miR-7b. We thus examined DNA methylation in the CpG islands in the *Hnrnpk* promoter region. Notably, DNA methylation levels in *K19-C2mE* gastritis and *Gan* mouse tumor tissues were not increased compared with the wild-type mouse stomach (Supplementary Figure 3a). Consistently, DNA methylation was not detected in the promoter region of the *HNRNPK* gene in human gastric cancer tissues (Figure 4a). We also examined the trimethylation of histone H3 at lysine 27 (H3K27me3) in

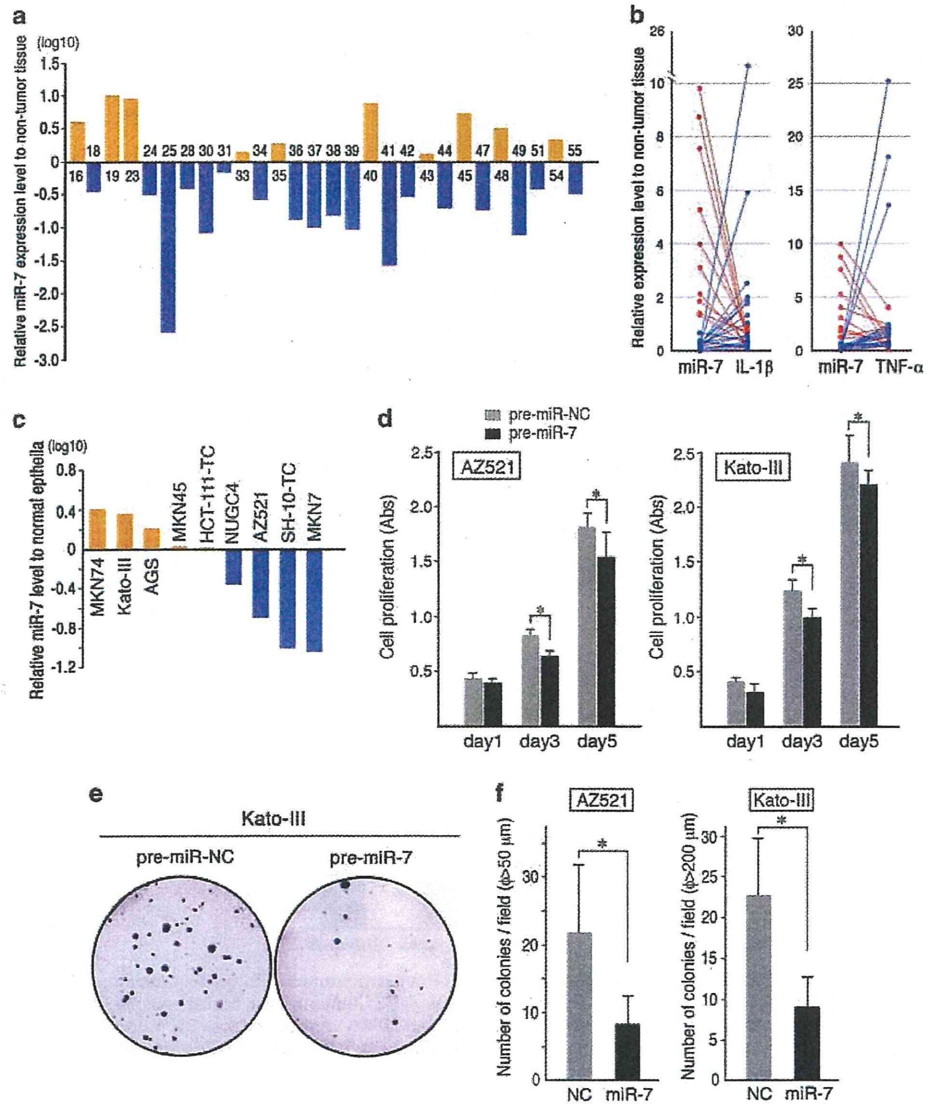

Figure 3 The tumor-suppressor roles of miR-7 in gastric cancer cells. (**a**) The relative miR-7 expression levels in the human gastric cancer tissue samples to the level of non-tumor stomach tissue samples are shown as the log10 ratios. The indicated numbers correspond to the patient ID in the clinicopathological data (Supplementary Table 3). (**b**) Comparison of the relative expression levels of miR-7 and IL-1β (left) or TNF-α (right) in gastric cancer tissues to the non-tumor stomach tissue levels in each patient is shown. Red and blue lines indicate that the expression of miR-7 was increased (>1.0) and decreased (<1.0) in the gastric cancers, respectively. (**c**) The relative expression levels of miR-7 in gastric cancer cell lines compared with the mean level in the human normal gastric epithelial cells are shown as the log10 ratios. The expression levels of miR-7 were normalized to those of U44. (**d**) The proliferation of control (gray bars) and pre-miR-7-transfected (closed bars) AZ521 cells and Kato-III cells at the indicated culture days are shown (mean ± s.d.). **P*<0.05. (**e**) Representative photographs of soft agar colonies in 6-well plates showing the pre-miR-NC- (left) and pre-miR-7-transfected (right) Kato-III cells. (**f**) The mean numbers of soft agar colonies larger than the indicated diameters in each well of 6-well plate of control (gray bars) and pre-miR-7-transfected (closed bars) AZ521 cells and Kato-III cells are shown (mean ± s.d.). **P*<0.05.

the upstream CpG islands of *Hnrnpk*. However, the H3K27me3 level was not increased in mouse gastritis and gastric tumors compared with the wild-type stomach (Figure 4b). These results indicate that DNA methylation and trimethylation of H3K27 are not involved in the downregulation of miR-7-1. Moreover, the genomic region including miR-7-1 was not deleted in human gastric cancer cells (Supplementary Figure 3b), suggesting that miR-7 downregulation in gastric cancer is not caused by genomic deletion.

We next examined whether activated macrophages have a role in the downregulation of miR-7, because the major source of proinflammatory cytokines in gastric tumors are macrophages (Oshima *et al.*, 2004, 2011). To monitor miR-7 activity, reporter vector-transfected cells were used. We confirmed that luciferase activity

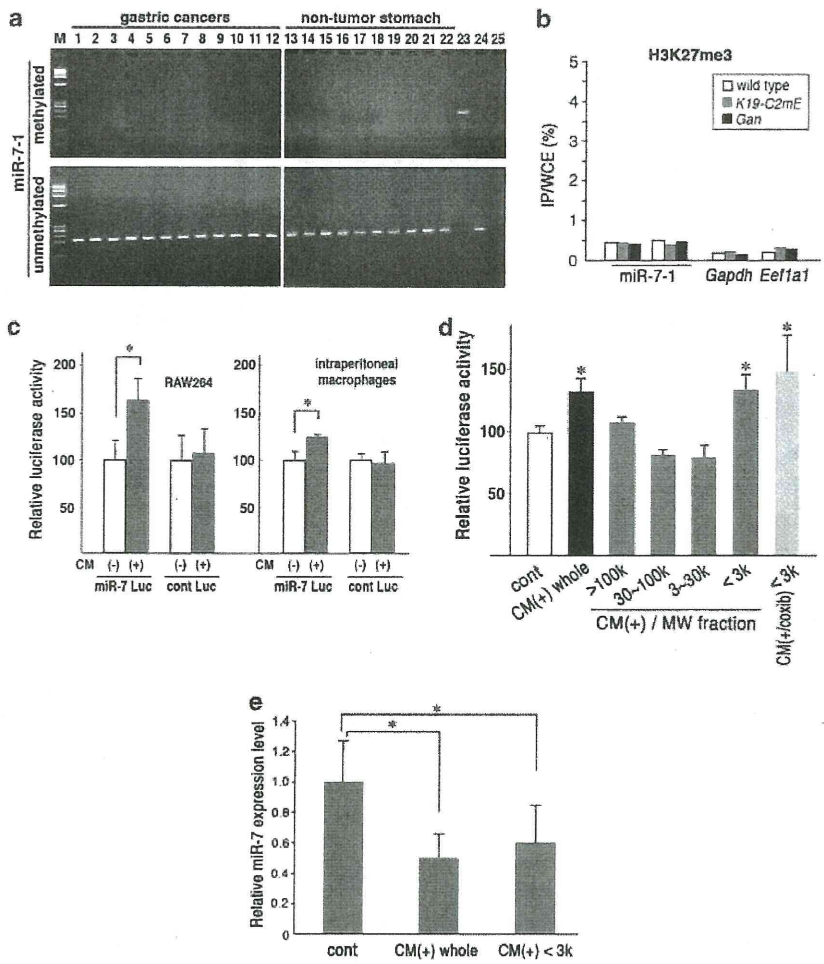

Figure 4 The mechanism responsible for the downregulation of miR-7 in gastric tumor cells. (**a**) Representative results of methylated (top) or unmethylated (bottom) status-specific PCR for miR-7-1. Lanes 1–12, human gastric cancer samples; lanes 13–22, non-tumor stomach samples; lane 23, methylated DNA control; lane 24, unmethylated DNA control; and lane 25, water control. (**b**) The results of ChIP-PCR analyses of miR-7-1 and the housekeeping genes, *Gapdh* and *Eef1a1*, for H3K27me3 in the gastric mucosa of respective genotype mice. The percentages of immunoprecipitated (*IP*)/whole-cell extracts (*WCE*) are shown for each primer set. (**c**) The luciferase activities of miR-7 Luc- or control Luc-transfected AZ521 reporter cells stimulated with CM(+) (gray bars) relative to those with CM(−) (open bars) are shown (mean ± s.d.). $^*P<0.05$. The conditioned medium was prepared from RAW264 cells (left) or intraperitoneal macrophages (right). (**d**) The luciferase activities of miR-7 Luc-transfected AZ521 reporter cells stimulated with whole CM(+) (closed bars), CM(+) fractionated to the indicated molecular sizes (gray bars), or fractionated CM(+) to <3 kDa collected from celecoxib-treated and LPS-stimulated macrophages (light gray bar) relative to the control level (open bar) are shown (mean ± s.d.). $^*P<0.05$ versus the control level. (**e**) The relative miR-7 expression levels examined by real-time RT–PCR in AZ521 cells stimulated with whole CM(+) or fractioned CM(+) <3 kDa relative to the control level are shown (mean ± s.d.). $^*P<0.05$ versus the control level. The expression levels of miR-7 were normalized to the U44 level.

was increased significantly when the miR-7 inhibitor was transfected into reporter vector-transfected Kato-III cells (Supplementary Figure 1c), indicating that the luciferase reporter system was working. Reporter cells were then treated with the conditioned medium of lipopolysaccharide-stimulated RAW264 cells (CM(+)) or unstimulated RAW264 cells (CM(−)). Importantly, the luciferase activity increased significantly when cells were stimulated with CM(+), whereas the luciferase activity was not changed in control vector-transfected cells (Figure 4c). Similar results were obtained when CM(+) and CM(−) were prepared using mouse intraperitoneal macrophages. These results indicate that activated macrophage-derived factor(s) caused miR-7 downregulation in gastric cancer cells.

To identify macrophage-derived factor(s) that suppress miR-7 expression, reporter cells were stimulated with TNF-α, IL-1β, IL-6 or PGE_2. However, none of these factors caused an increase in luciferase activity (Supplementary Figure 4). We thus fractionated CM(+) by ultrafiltration, and separated by molecular weight. Interestingly, a CM(+) fraction of <3 kDa significantly increased the luciferase activity to a similar level as that induced by whole CM(+), whereas the other CM(+) fractions did not (Figure 4d). Moreover, the luciferase activity was still increased when CM(+)

was prepared under co-treatment of RAW264 cells with lipopolysaccharide and a COX-2 inhibitor, celecoxib. We confirmed the decreased level of miR-7 by real-time RT–PCR in CM(+)- or CM(+) fraction <3 kDa-treated AZ521 cells (Figure 4e). These results indicate that small molecule(s) (<3 kDa) derived from activated macrophages are responsible for miR-7 repression in gastric cancer cells, and that such small molecule(s) are expressed in activated macrophages in a COX-2/PGE_2-independent manner.

Downregulation of miR-7 in the stomach by inflammatory responses

We next examined whether inflammatory responses are responsible for miR-7 downregulation in the stomach using different mouse models. The stomachs of wild-type mice were infected with *Helicobacter felis*, and submucosal inflammatory infiltration and mucosal macrophage accumulation were confirmed at 20 weeks after the infection (Figures 5a and b). Notably, the miR-7 expression level was significantly decreased in the *H. felis*-infected inflamed gastric mucosa (Figure 5c).

We recently showed that inflammatory responses and macrophage infiltration were suppressed in *K19-C2mE* mouse gastritis and *Gan* mouse tumors when mice were maintained under germfree conditions (Figure 5d and Oshima *et al.*, 2011). Notably, miR-7 expression levels were increased significantly in germfree *K19-C2mE* and *Gan* mice compared with the levels of mice maintained in a specific pathogen free (SPF) facility (Figure 5e). These *in vivo* experiments suggest that inflammatory responses are responsible for the miR-7 downregulation in the stomach, although further genetic studies are required to examine the role of macrophages in miR-7 downregulation.

Inflammation-dependent upregulation of miR-7 target genes in gastric tumors

The epidermal growth factor receptor (*EGFR*) mRNA is one of the miR-7 target genes (Kefas *et al.*, 2008;

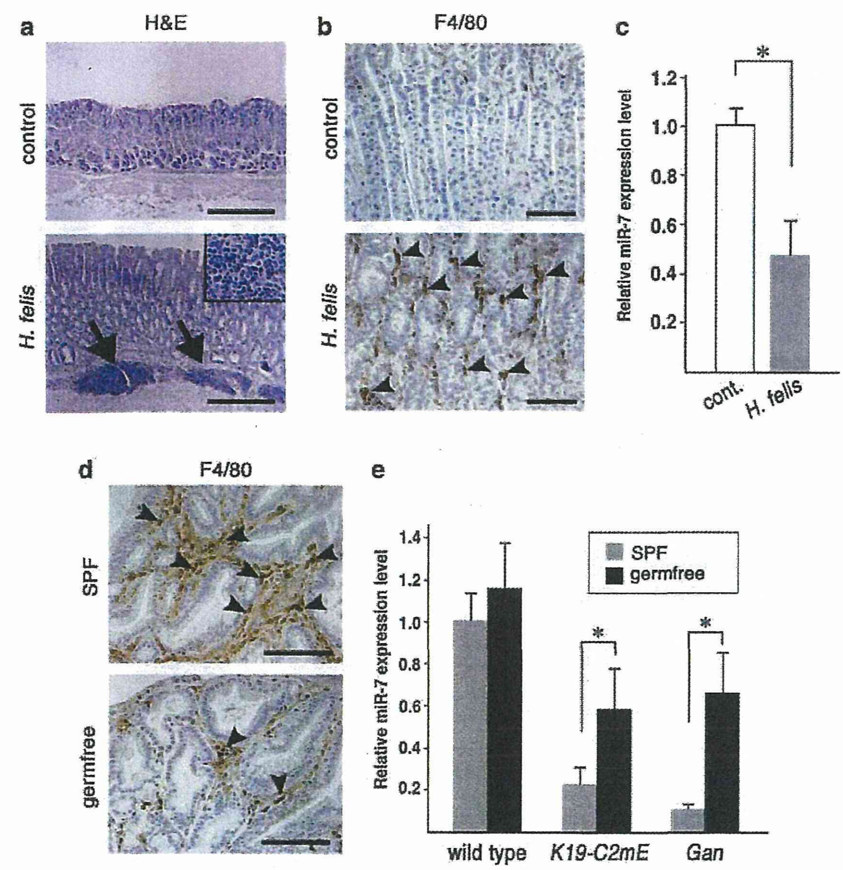

Figure 5 Inflammation-induced miR-7 repression in the mouse stomachs. (**a**) Histology of the wild-type mouse normal glandular stomach (top) and *H. felis*-infected inflamed glandular stomach (bottom). Arrows and inset indicate submucosal inflammatory cell infiltration. Scale bars indicate 0.5 mm. (**b**) Immunostaining of F4/80 in the normal glandular stomach (top) and *H. felis*-infected glandular stomach (bottom). Arrowheads indicate macrophages. Scale bars indicate 100 μm. (**c**) The miR-7 expression level of *H. felis*-infected gastric mucosa (gray bar) relative to that of the control stomach (open bar) is shown (mean ± s.d.). $*P<0.05$. (**d**) Immunostaining of F4/80 in a SPF control *Gan* mouse tumor (top) and a germfree *Gan* mouse tumor (bottom). Arrowheads indicate macrophages. Scale bars indicate 100 μm. (**e**) The expression levels of miR-7 in SPF (gray bars) and germfree (closed bars) K19-*C2mE* mouse gastritis and *Gan* mouse gastric tumors relative to the SPF wild-type stomach levels are shown (mean ± s.d.). $*P<0.05$. The expression levels of miR-7 were normalized to the Sno202 level.

Webster *et al.*, 2009). We thus examined *EGFR* expression levels in pre-miR-7-transfected Kato-III and AZ521 gastric cancer cells. As expected, the *EGFR* expression level was decreased significantly by pre-miR-7 transfection in both cell lines (Figure 6a), suggesting that suppression of *EGFR* expression is one of the tumor-suppressor mechanisms of miR-7 against gastric cancer development.

To identify novel miR-7 target genes that are upregulated in the inflammatory microenvironment,

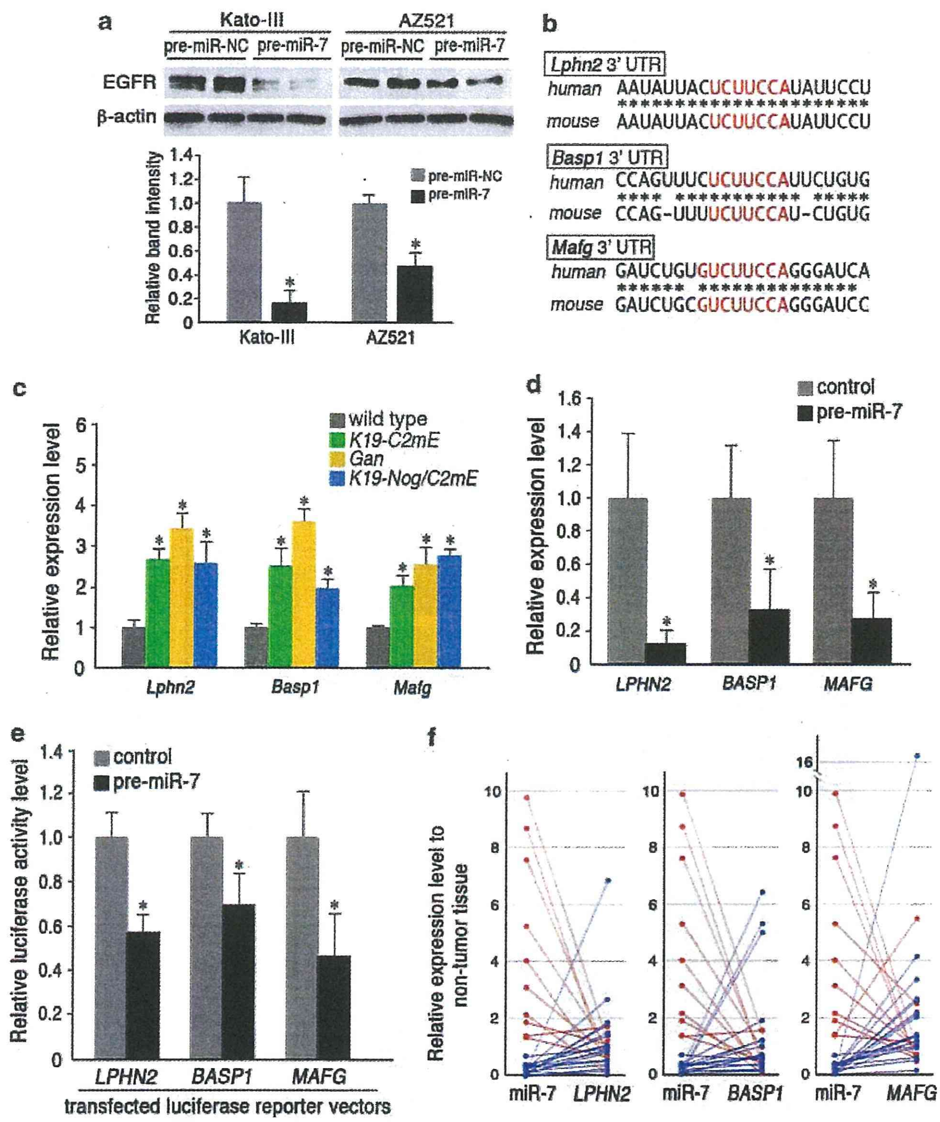

Figure 6 Inflammation-dependent upregulation of miR-7 target genes. (**a**) Representative results of the western blotting analysis of EGFR in Kato-III cells (top left) and AZ521 cells (top right) transfected with pre-miR-NC and pre-miR-7. The results for two independently prepared samples are shown. β-Actin was used as an internal control. The relative band intensities of the western blotting results are shown in the bar graph (mean ± s.d.) (bottom). *$P<0.05$ versus the control level. (**b**) Alignment of the miR-7 target sequences in the 3′-UTR of *Lphn2*, *Basp1* and *Mafg* in human and mouse mRNAs. The seed match sequences for miR-7 are indicated in red. (**c**) The expression levels of the indicated genes in *K19-C2mE* mouse gastritis (green bars), *Gan* mouse gastric tumors (yellow bars) and *K19-Nog/C2mE* mouse gastric hamartomas (blue bars) relative to the wild-type levels (gray bars) are shown (mean ± s.d.). *$P<0.05$ versus the wild-type level. The results were extracted from the microarray data set (Gene Expression Omnibus (GEO), accession GSE16902). (**d**) The expression levels of the indicated genes examined by real-time RT–PCR in pre-miR-7-transfected Kato-III cells (closed bar) relative to those of the control cells (gray bar) are shown (mean ± s.d.). *$P<0.05$ versus control level. (**e**) The relative luciferase activity levels of pre-miR-7-transfected reporter cells (closed bars) to the levels of control pre-miR-NC-transfected reporter cells (gray bars) are shown. The target genes for the respective luciferase reporter vectors are indicated. *$P<0.05$ versus the control level. (**f**) Comparison of the relative expression levels of miR-7 and *LPHN2* (left), *BASP1* (center) or *MAFG* (right) in human gastric cancers with non-tumor stomach levels is shown. Red and blue lines indicate that miR-7 was increased (>1.0) and decreased (<1.0) in gastric cancers, respectively. The expression levels of miR-7 were normalized to the U44 level.

we searched for putative miR-7 target genes from the upregulated gene set in both *K19-C2mE* mouse gastritis and *Gan* mouse gastric tumors using the results of the microarray analyses (Itadani *et al.*, 2009). We found that the *Lphn2*, *Basp1* and *Mafg* genes have conserved miR-7 target sequences in their 3′ untranslated region in both mouse and human mRNAs (Figure 6b). Notably, the expression of these genes was significantly increased not only in *K19-C2mE* mouse gastritis and *Gan* mouse tumors but also in *K19-Nog/C2mE* mouse gastric hamartomas (Figure 6c). The gastric mucosa and tumors in these strains are inflamed as a result of induction of the COX-2/PGE_2 pathway (Oshima *et al.*, 2004, 2006, 2009), suggesting that downregulation of miR-7 in inflammatory lesions is involved in upregulation of these genes. Notably, transfection of pre-miR-7 into Kato-III cells resulted in a significant decrease of *LPHN2*, *BASP1* and *MAFG* expressions (Figure 6d). Moreover, we constructed luciferase reporter plasmids that contained the 3′ untranslated region fragment of the putative miR-7 target genes, and transfected these vectors into Kato-III cells. Consistent with the real-time RT–PCR results, luciferase activities of reporter vector-transfected cells decreased significantly when cells were co-transfected with pre-miR-7 (Figure 6e). Taken together, these results indicate that these three genes are miR-7 targets.

Finally, we examined the expressions of *LPHN2*, *BASP1* and *MAFG* in human gastric cancers by real-time RT–PCR and compared their expressions with miR-7 expression levels. We found that expression levels of miR-7 and *LPHN2*, *BASP1* and *MAFG* were inversely correlated (Figure 6f). Accordingly, it is possible that inflammation causes induction of these genes in human gastric cancers through downregulation of miR-7, which may contribute to gastric tumorigenesis, although this will need to be investigated in future studies.

Discussion

It has been shown that miR-155 and miR-21, which function as oncogenes, are induced by inflammatory pathways, providing a link between inflammation and cancer (O'Connell *et al.*, 2007; Tili *et al.*, 2007; Iliopoulos *et al.*, 2010). Consistently, we found inflammation-dependent induction of miR-155 and miR-21 in mouse gastric tumors. On the other hand, miR-145 and miR-7, which function as tumor suppressors, are downregulated in both mouse gastritis and gastric tumor tissues. Moreover, we found that miR-7 levels are inversely correlated with the levels of proinflammatory cytokines, suggesting that the severity of inflammatory response is related to miR-7 downregulation. Therefore, it is possible that inflammation can promote tumorigenesis both by the upregulation of oncogenic miRNAs and by the downregulation of tumor-suppressor miRNAs, possibly through different mechanisms. Such alterations of cancer-related miRNA expression likely link inflammation and cancer.

It has been reported that miR-7 has a tumor-suppressor role in various cancers including brain tumors, breast cancer and lung cancer (Kefas *et al.*, 2008; Reddy *et al.*, 2008; Webster *et al.*, 2009), and we herein showed that miR-7 also functions as a tumor suppressor in gastric cancer. Interestingly, in the normal stomach, miR-7 expression is induced during the differentiation of gastric epithelial cells, suggesting a role of miR-7 in the regulation of epithelial cell differentiation. It has also been reported that miR-7 expression is induced during differentiation of intestinal epithelial cells (Nguyen *et al.*, 2010) and cortical neurons (Chen *et al.*, 2010). These results collectively suggest that miR-7 has a role in regulating cell differentiation in various organs. Therefore, it is conceivable that suppression of miR-7 expression is required for maintenance of the undifferentiated status of stem or progenitor cells in these organs.

These results suggest the possibility that inflammation suppresses epithelial cell differentiation through repression of miR-7. It is not surprising that the inflammatory response suppresses cell differentiation and enhances proliferation when regeneration is required in injured tissues. It has also been shown that a disruption of Toll-like receptor signaling causes an impairment of tissue repair by intestinal epithelial cells (Rakoff-Nahoum *et al.*, 2004). Moreover, activated macrophages are important niche components for intestinal epithelial progenitors in regenerative responses (Pull *et al.*, 2005). Therefore, it is conceivable that downregulation of miR-7 leads to suppression of differentiation, inducing the proliferation of undifferentiated epithelial cells in the inflammatory microenvironment.

Although several target genes of miR-7 have been identified, it is still unclear how miR-7 regulates differentiation. *EGFR* is one of the important miR-7 target genes, and is at least partially responsible for its tumor-suppressor role (Kefas *et al.*, 2008). Moreover, p21-activated kinase 1, Raf1, and the insulin-like growth factor 1 receptor have also been identified as miR-7 target genes that are upregulated in cancer cells (Reddy *et al.*, 2008; Webster *et al.*, 2009; Jiang *et al.*, 2010). Although most of these gene products contribute to cancer cell proliferation, we believe that miR-7 inhibits expression of other factors that have a role in the maintenance of the undifferentiated status of epithelial cells. In this study, we identified three novel miR-7 target genes that are upregulated in gastric cancers in an inflammation-dependent manner. LPHN2 is a G protein-coupled receptor that binds α-latrotoxin (Ichtchenko *et al.*, 1999), whereas BASP1 is implicated in neurite outgrowth (Korshunova *et al.*, 2008). MAFG is one of the small Maf proteins that is important for antioxidant responses (Katsuoka *et al.*, 2005). Although it remains to be investigated, it is of interest to examine whether these molecules have any role in the differentiation or tumorigenesis of gastric epithelial cells.

We examined the mechanisms responsible for miR-7 downregulation in gastric tumor cells. *Helicobacter pylori* infection induces chronic gastritis, resulting in induction of DNA methylation (Niwa *et al.*, 2010). The expression of miR-34b/c is suppressed by DNA methylation in *H. pylori*-associated gastric cancer cells (Suzuki *et al.*, 2010). Moreover, H3K27me3 leads to tumor-suppressor gene silencing in cancer (Kondo *et al.*, 2008). However, we showed that downregulation of miR-7 is not caused by genomic deletion nor by epigenetic mechanisms, but through stimulation by macrophage-derived factor(s). Several mechanisms for the regulation of miR-7 expression have been reported. For example, miR-7 transcription is directly induced by HoxD10 (Reddy *et al.*, 2008) or c-Myc (Chou *et al.*, 2010). Splicing factor SF2/ASF binds the pri-miR-7 to enhance its cleavage by Drosha (Wu *et al.*, 2010). Accordingly, it is conceivable that macrophage-derived molecule(s) directly downregulate miR-7 expression or indirectly suppress miR-7 expression through modulation of these regulation systems. The identification of responsible macrophage-derived molecule(s) will provide a novel mechanism by which macrophages promote tumorigenesis.

In conclusion, we showed that inflammation simultaneously induces upregulation of oncogenic miRNAs and downregulation of tumor-suppressor miRNAs, which promote tumorigenesis. The expression of miR-7 is induced during differentiation of gastric epithelial cells, suggesting a role for miR-7 in the regulation of epithelial cell differentiation. Accordingly, it is possible that the downregulation of miR-7 contributes to suppression of differentiation, resulting in the promotion of gastric tumorigenesis. Moreover, small molecule(s) expressed by activated macrophages are responsible for miR-7 repression, providing a link between inflammation and cancer. Therefore, miR-7 may be useful for devising a new preventive or therapeutic strategy against gastric cancer through the induction of cancer cell differentiation.

Materials and methods

Mouse models

Construction of *K19-C2mE* and *Gan* (*K19-Wnt1/C2mE*) mice was described previously (Oshima *et al.*, 2004, 2006). In brief, *K19-C2mE* mice express *Ptgs2* and *Ptges* in gastric epithelial cells, whereas *Gan* mice express *Ptgs2*, *Ptges* and *Wnt1*. For expression analyses, *K19-C2mE* mouse gastritis and *Gan* mouse gastric tumor samples, and wild-type mouse stomach tissues were obtained at 30–40 weeks of age. Germfree mouse colonies were constructed as described previously (Oshima *et al.*, 2011), and the histology and miR-7 expression were examined at 55 weeks of age ($n = 5$). *H. felis* (American Type Culture Collection 49179, ATCC, Manassas, VA, USA) were inoculated at 10^8 per mouse into wild-type mice at 6–8 weeks of age, and the histology and miRNA expression were examined at 20 weeks after infection ($n = 6$). All animal experiments were carried out according to a protocol approved by the Committee on Animal Experimentation of the Kanazawa University.

Microarray analysis

Total RNA was extracted from mouse stomachs ($n = 3$) using ISOGEN (Nippon Gene, Tokyo, Japan), pooled with the same genotype mouse RNAs, labeled with Cy3 and hybridized to Mouse miRNA microarray Rel. 12.0 (Agilent Technologies, Santa Clara, CA, USA). The raw data were normalized using the GeneSpring GX software program (Agilent Technologies), and expression levels of miRNAs in gastritis and gastric tumor tissues were compared with those in the wild-type mouse stomach. Transcripts with low signals (less than threefold of the background level) were not used for further analyses. The expression of miRNAs was further examined by real-time RT–PCR using RNA samples independently prepared from a different set of wild-type, *K19-C2mE* and *Gan* mice ($n = 5$ for each genotype).

The results of cDNA microarray data sets of *K19-C2mE*, *Gan* and *K19-Nog/C2mE* mice were deposited into the Gene Expression Omnibus, as accession number GSE16902 (Itadani *et al.*, 2009), and were searched for the presence of novel miR-7 target genes using the TargetScan 5.1 program (MIT, Cambridge, MA, USA) (http://www.targetscan.org).

Real-time RT–PCR

Paired gastric cancer and non-tumor stomach tissue samples were obtained from 28 patients during surgery at the Kanazawa University Hospital, Japan. Fresh frozen tissues were used for expression analyses. Clinicopathological data of patients are shown in Supplementary Table 3. Human normal gastric epithelial cells were prepared by isolating the gastric glands from normal stomach tissues ($n = 4$) as described previously (Cheng *et al.*, 1984). Approval for this project was obtained from the Kanazawa University Medical Ethics Committee, and written informed consent was obtained before specimen collection. Mouse stomachs were obtained from E15 wild-type mouse embryos, and day 0, day 7, day 14 and adult mice ($n = 3$ for each). Total RNAs were extracted from tissues or cells using ISOGEN (Nippon Gene), and cDNAs for miRNAs and mRNAs were constructed using QuantiMir RT kit (System Bioscience, Mountain View, CA, USA) and the PrimeScript RT reagent Kit (Takara, Tokyo, Japan), respectively. Real-time RT–PCR was performed using SYBR Premix Ex TaqII (Takara, Tokyo, Japan) and Stratagene Mx3000P (Agilent Technologies). Sno202 and U44 were used as endogenous miRNA controls for mice and humans, respectively, whereas β-actin was used for endogenous mRNA control. The primer sequences for the miRNAs are shown in Supplementary Table 4. The primers for mRNAs were purchased from Takara.

Cell culture experiments

Mouse glandular stomachs were treated with 0.1% collagenase for 30 min at 37 °C, followed by centrifugation at 20 *g* for 3 min to isolate gastric glands. For the primary culture, isolated gastric glands were digested with trypsin and seeded on collagen-coated dishes as described previously (Oshima *et al.*, 2004). On day 2, the primary cultured cells were treated with 10 mM EDTA-phosphate-buffered saline and passaged. The primary cultured cells on day 2 (P0) and day 6 (P1) were used for the expression analysis. Human gastric cancer cell lines, AGS (ATCC), AZ521, MKN74, MKN45, NUGC4, HCT-111-TC, SH-10-TC (RIKEN BioResource Center, Tsukuba, Japan), Kato-III and MKN7 (Cell Resource Center for Biomedical Research, Tohoku University, Japan) were used in this study.

The pre-miR miRNA-7 (Pre-miR-7), pre-miR negative control (Pre-miR-NC) and anti-miR-7 inhibitor (Ambion, Austin, TX, USA) were used for transfection. The cell proliferation rate was measured using the Cell Counting Kit-8 (Dojindo, Kumamoto, Japan). For the soft agar colony